

What the Gribov copy tells on the confinement and the theory of dynamical chiral symmetry breaking

Sadataka Furui

School of Science and Engineering, Teikyo University, 320-8551 Japan.

Hiroyuki Nakajima^y

Department of Information Science, Utsunomiya University, 321-8585 Japan.

(Dated: December 25, 2018)

We performed lattice Landau gauge QCD simulation on $= 6.0; 16^4; 24^4; 32^4$ and $= 6.4; 32^4; 48^4$ and 56^4 by adopting the gauge fixing that minimizes the norm of the gauge field, and measured the running coupling by using the gluon propagator and the ghost propagator. It has a maximum $s(q) \approx 1.1$ at around $q = 0.5$ GeV and decreases as q approaches 0, and the Kugo-Ojima parameter reached -0.83. The infrared exponent of the ghost propagator is $= 0.2$ in the gauge fixing, but in 56^4 there is an exceptional configuration $= 0.27$, and the running coupling using this configuration is consistent with the Dyson-Schwinger approach with infrared fixed point ≈ 1.5 .

The features of the exceptional configuration are investigated by measuring one-dimensional Fourier transform (1-d FT) of the gluon propagator transverse to 4 lattice axes. We observe that the 1-d FT along a specific axis of the exceptional configuration violates reflection positivity and the average of the Cartan subalgebra components of the Kugo-Ojima parameter along this axis is consistent to -1.

PACS numbers: 12.38.Gc, 11.15.Ha, 11.15.Tk

I. INTRODUCTION

The lattice Landau gauge QCD simulation suffers from Gribov copy problem and its effect on the confinement was discussed by many authors [1, 2, 3, 4]. We adopted the fundamental modular gauge fixing and studied the Gribov copy problem in $SU(2)$ and $SU(3)$ [5] and observed that the configuration possessing the minimum norm does not necessarily have the horizon function deviation factor h small, i.e. not close to the continuum limit of the fundamental modular region. The Kugo-Ojima parameter which gives the sufficient condition of the confinement [6] was measured and the parameter of a sample with the minimum norm was not closer to -1 than that of the first copy.

In the previous paper [7], we measured the QCD running coupling and the Kugo-Ojima parameter in $= 6.0; 16^4; 24^4; 32^4$ and $= 6.4; 32^4$ and 48^4 . The running coupling was found maximum of about 1.1 at around $q = 0.5$ GeV, and behaves either approaching constant or even decreasing as q approaches zero, and the Kugo-Ojima parameter was getting larger but staying around

0.8 in contrast to the expected value -1 in the continuum theory. Thus it is necessary to perform a larger lattice simulation and to study the dependence of the Gribov copy, and analyse the lattice data by comparing with continuum theory like Dyson-Schwinger equation (DSE).

There are extensive reviews on DSE for the Yang Mills

theory [8, 9, 10]. The solution of DSE depends on ansatz of momentum truncation and what kind of loop diagrams are included. Two decades ago Mandelstam [11] projected the DSE for the gluon propagator by $P(q) = q \cdot q = q^2$ and without including ghosts, assumed the gluon wavefunction renormalization factor in the form

$$Z(q^2) = \frac{b}{q^2} + C(q^2) \quad b = \text{const.} \quad (1)$$

Later Brown and Pennington [12] argued that in order to decouple divergent tadpole contribution, it is more appropriate to project the gluon propagator by $R(q) = 4q \cdot q = q^2$. A careful study of inclusion of ghost loop in this DSE was performed by [13], and they showed the infrared QCD running coupling in Landau gauge could be finite.

The divergent QCD running coupling caused difficulty in the model building of dynamical chiral symmetry breaking [14, 15]. In order to get reasonable values of the quark condensates, infrared finite QCD running coupling was favored. Recent DSE approach with multiplicative renormalizable (MR) truncation with infrared finite QCD running coupling [16, 17] suggests that the confinement and the chiral symmetry breaking can be explained by the unique running coupling. We thus compare the running coupling obtained from our lattice simulation and that used in the DSE and study the dependence on the Gribov copy.

We produced $SU(3)$ gauge configurations by using the heat-bath method, performed gauge fixing and analyzed lattice Landau gauge configurations of $= 6.4, 56^4$. The $= 6.4; 48^4$ and 56^4 lattices allow measuring the ghost propagator in the momentum range $[0.48, 14.6]$ GeV, and $[0.41, 14.6]$ GeV, respectively. In the present work, the

Electronic address: furui@umb.teikyo-u.ac.jp;
URL: http://albert.umb.teikyo-u.ac.jp/furui_lab/furuipbs.htm
Electronic address: naka@is.utsunomiya-u.ac.jp

gauge field is defined from the link variables as $\log U$ type:

$$U_{x_i} = e^{A_{x_i}}; A_{x_i}^y = A_{x_i};$$

The fundamental modular gauge fixing (FMG) [2] of lattice size L is specified by the global minimum along the gauge orbits, i.e.,

$L = f_U f_U (1) = M \log f_U (g) g$, $L = L$, where L is called the Gribov region (local minimum) and

$$L = f_U j \cdot \partial U = 0; \partial A (U) = 0 g;$$

Here $f_U (g)$ is defined as

$$f_U (g) = \frac{1}{(n^2 - 1)4V} \sum_x \text{tr} A_{x_i}^g A_{x_i}^y; \quad (1)$$

In the gauge transformation

$$e^{A_{x_i}^g} = g_x^y e^{A_{x_i}}; g_{x_i}^y; \quad (2)$$

where $g = e$, the value is chosen depending on the maximum norm $\|\partial A\|_{\infty}$ as follows.

$$\text{When } \|\partial A\|_{\infty} > \|\partial A\|_0: x = \frac{0}{k \|\partial A\|_0} \partial A_x \quad (1 < 0 < 2.2) \quad (3)$$

$$\text{When } \|\partial A\|_{\infty} < \|\partial A\|_0: = (\partial D (A))^{-1} \partial A \quad (1 < 2) \quad (4)$$

In the second case, calculation of $(\partial D (A))^{-1}$ is performed by Newton's method where the linear equation is solved up to third order of the gauge field, and then the Poisson equation is solved by the multigrid method [18, 19, 20]. The accuracy of the gauge fixed configuration characterized by $\partial A (U) = 0$ is 10^{-4} in the maximum norm which turned out to be about 10^{-15} in the L_2 norm of the gauge field in contrast to about 10^{-12} in 48^4 .

In the calculation of the ghost propagator, i.e. inverse Faddeev-Popov (FP) operator, we adopt the conjugate gradient (CG) method, whose accuracy of the solution in the $q < 0.8G$ eV region turned out to be less than 5% in the maximum norm [5, 7].

In [7], we analyzed these data using a method inspired by the principle of minimal sensitivity (PMS) and/or the effective charge method [21, 22], the contour-improved perturbation method [23] and the DSE approach [9, 13]. We perform the same analysis to the 56^4 data.

The infrared behavior of the running coupling is tightly related to the mechanism of the dynamical chiral symmetry breaking [15, 16, 24]. The lattice data are compared with the theory of dynamical chiral symmetry breaking based on the DSE.

In sec. II we show some details of the gauge fixing procedure and show sample dependence of the gluon propagator, Kugo-Ojima parameter and QCD running coupling. In sec. III a brief summary of the DSE as well as the recent exact renormalization group approach (ERGE) are presented. We compare lattice data with results of the theoretical analysis of DSE. Issues on dynamical chiral symmetry breaking is discussed in sect IV.

II. GRIBOV COPY AND THE 56^4 LATTICE DATA

The magnitude of $\|\partial A\|_{\infty}$ in the gauge transformation is chosen to be 2.2 (copy A) or 2 (copy B) i.e. larger or smaller than 2 = 3. In most cases, gauge fixed configurations are almost the same, but in some cases, different $\|\partial A\|_{\infty}$ produce significantly different copies.

In order to see the difference of the gluon field of the Gribov copies, we measured the 1-dimensional Fourier transform (1-d FT) of the gluon propagator transverse to the lattice coordinate axes. It is equivalent to the specific Schwinger function

$$S(t; 0) = \frac{1}{L} \sum_{q_0=0}^{L-1} D_A(q_0; 0) e^{i q_0 t} \quad (3)$$

where L is the lattice size. Here the function $D_A(q^2)$ is defined as

$$D_A(x; q) = \frac{1}{n^2 - 1} \sum_{x=x_i, t}^X e^{i q x} \text{Tr} h A(x) A(0)^y i \\ = \left(-\frac{q \cdot q}{q^2} \right) D_A(q^2); \quad (4)$$

When the Schwinger function becomes negative, the reaction positivity becomes violated, which means that the gluon is not a physical particle. Violation of positivity is considered as a sufficient condition of the confinement [9, 24, 25].

The four 1-d FT of the sample I_A and those of the sample I_B are shown in Fig. 1 and in Fig. 2, respectively. The solid line, dotted line, dashed line and the dash-dotted line corresponds to propagator transverse to x_1, x_2, x_3 and x_4 axis in the Euclidean space, respectively.

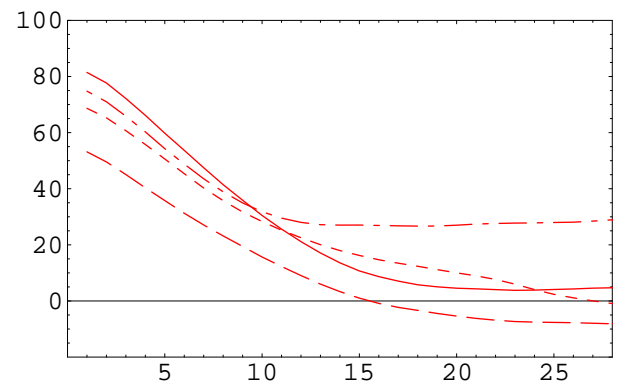


FIG. 1: The 1-d FT of the gluon propagator along the 4 axes. $= 64, 56^4$ in the $\log U$ version. sample I_A

We observe that the gluon propagator of sample I_A has a specific symmetry, i.e. one propagator manifestly violates reaction positivity and one propagator almost

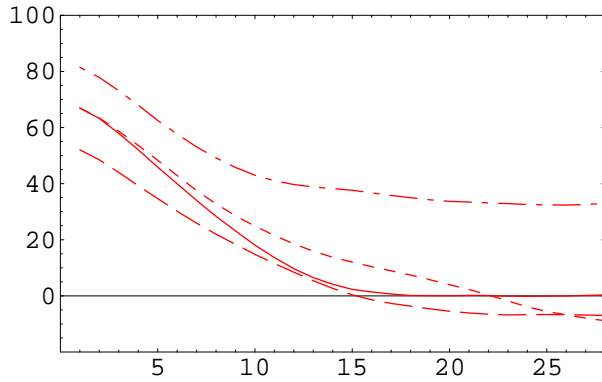


FIG. 2: The 1-d FT of the gluon propagator along the 4 axes. $= 64,56^4$ in the log U version. sample I_B

parallel to it remains finite. In the sample I_B , the propagator that manifestly violates reaction positivity does not change but other propagators are shifted and especially the propagator which was parallel in I_A becomes almost 0 in the large distance. Here, manifestly means it remains negative in a wide range in the intermediate not only near the right edge of the coordinate.

The ghost propagator is defined by the expectation value of the inverse Faddeev-Popov (FP) operator M

$$D_G^{ab}(x; y) = \langle h^a x j[M]^{-1} j^b y \rangle; \quad (5)$$

via the Fourier transform

$$D_G(q^2) = \frac{G(q^2)}{q^2}; \quad (6)$$

The Kugo-Ojima parameter is defined by the two point function of the covariant derivative of the ghost and the commutator of the antighost and gauge field

$$\begin{aligned} & \left(-\frac{q \cdot q}{q^2} \right) u^{ab}(q^2) \\ &= \frac{1}{V} \sum_{x,y} e^{i p(x-y)} \text{tr} \left[\frac{1}{\partial D} [A^a; \partial^b] \right]_{xy} \quad (7) \end{aligned}$$

We performed the same analyses as sample I for a sample which has the second largest Kugo-Ojima parameter (samples II_A and II_B). The sample dependences of the L_2 norm of the gauge field, Kugo-Ojima parameter $c = u(0)$, trace divided by the dimension $e=d$, horizon function deviation parameter h [2, 18] and the infrared exponent of the ghost propagator ζ which is equal to ζ_D are summarized in Table I. In the average, sample A are incorporated. The number of gauge fixed samples of the 56^4 lattice is 15.

We observed that in most samples the dependence of the copy on ζ_A is weak as in the case of sample II, and that the large difference of I_A and I_B copies is exceptional. The Table I also shows that ζ , c and h are correlated. The ζ of the sample average is 0.22, but

that of the I_A copy is 0.27. The I_A copy has a larger L_2 norm of the gauge field but smaller h and larger c . We find that not all samples have the axis that manifestly violates reaction positivity and that the direction of the axis is sample dependent.

A. Kugo-Ojima parameter

Our sample average of $c = u(0)$, $e=d$, h , ζ_G and the exponent of the gluon dressing function near zero momentum ζ_D and near $q = 1.97 \text{ GeV}$ are summarized in Table II.

The color off-diagonal, space diagonal part of the Kugo-Ojima parameter c was 0.0001 (162) and consistent to 0. The magnitude of the Kugo-Ojima parameter c and exponent of the ghost propagator ζ_G are tightly correlated and they are also correlated with the violation of the reaction positivity in the gluon propagator. In the I_A copy, reaction positivity is violated along x_3 axis and the average of 33 and 88 components of c along this axis is 0.97, consistent to 1.

B. Gluon propagator

The gluon propagator in momentum space was measured by using cylindrical cut method [26], i.e., choosing momenta close to the diagonal direction. In Fig. 3 we show the gluon dressing function of $= 64,56^4$ lattice data together with 48^4 lattice data. The gluon propagators of 24^4 , 32^4 and 48^4 as a function of the physical momentum agree quite well with one another and they can be fitted by the $\hat{M}^* \text{OM}$ scheme [7].

$$D_A(q^2) = \frac{Z(q^2; y)_{y=0.02227}}{q^2} = \frac{Z_A(q^2)}{q^2} \quad (8)$$

in the $q > 0.8 \text{ GeV}$ region.

C. Ghost propagator

The ghost dressing function is defined by the ghost propagator as $G^{ab}(q^2) = q^2 D_G^{ab}(q^2)$. In Fig. 4, $= 64$,

TABLE I: The Gribov copy dependence of the Kugo-Ojima parameter c , trace divided by the dimension $e=d$, horizon condition deviation parameter h and the exponent ζ_G .

	I_A	I_B	II_A	II_B	average
$k_A k^2$	0.09081	0.09079	0.090698	0.090695	0.09072 (7)
c	0.851 (77)	0.837 (58)	0.835 (53)	0.829 (56)	0.827 (15)
$e=d$	0.9535	0.9535	0.9535	0.9535	0.954
h	-0.102	-0.117	-0.118	-0.125	-0.127
ζ	0.272	0.241	0.223	0.221	0.223

TABLE II: The Kugo-Ojima parameter c , trace divided by the dimension d , horizon function deviation h in the $\log U$ version. The exponent of the ghost dressing function near zero momentum γ_g , the exponent of the gluon dressing function near zero momentum γ_d , near $q = 1.97 \text{ GeV}$ in $\log U$ type. $\gamma_g = 6.0$ and 6.4 .

L	6.0			6.4		
	16	24	32	32	48	56
c	0.628(94)	0.774(76)	0.777(46)	0.700(42)	0.793(61)	0.827(27)
γ_d	0.943(1)	0.944(1)	0.944(1)	0.953(1)	0.954(1)	0.954(1)
h	-0.32	-0.17	-0.16	-0.25	-0.16	-0.12
γ_g	0.175	0.175	0.174	0.174	0.193	0.223
γ_d^0		-0.310	-0.375		-0.273	-0.323
γ_d^0	0.38	0.314	0.302	0.31	0.288	0.275

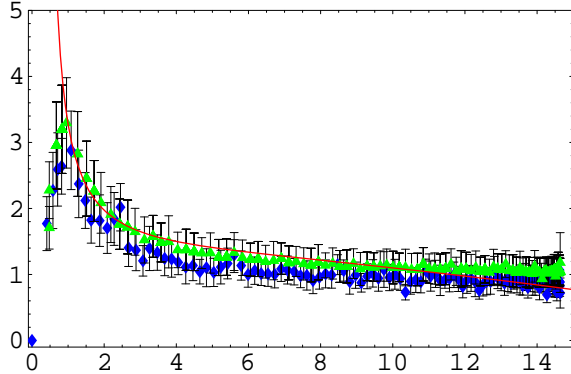


FIG. 3: The gluon dressing function as the function of the momentum $q(\text{GeV})$. $\gamma_d = 6.4$, 48^4 (stars) and 56^4 (diamonds) in the $\log U$ version. The solid line is that of the $\hat{\text{MOM}}$ scheme.

48^4 , and 56^4 and $\gamma_d = 6.0$ 24^4 and 32^4 lattice data of the ghost dressing function are compared with that of the $\hat{\text{MOM}}$ scheme [7, 27]

$$D_G(q^2) = \frac{Z_g(q^2; y)_{y=0.02142}}{q^2} = \frac{G(q^2)}{q^2} : \quad (9)$$

We observe that the agreement is good for $q > 0.5 \text{ GeV}$. The ghost propagator was first measured in [28] but the scaling property was not observed and the lowest momentum point was incorrectly suppressed.

D. QCD running coupling

We measured the running coupling from the product of the gluon dressing function and the ghost dressing function squared [13]. We parametrize infrared power dependence of $D_A(q^2)$ as $\propto (qa)^{2(1+\gamma_d)}$ and that of $D_G(q^2)$

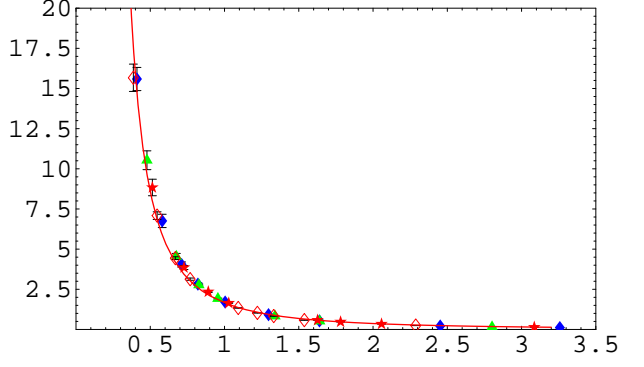


FIG. 4: The ghost propagator as the function of the momentum $q(\text{GeV})$. $\gamma_d = 6.0$, 24^4 (star), 32^4 (unfilled diamond), $\gamma_d = 6.4$, 48^4 (triangle) and 56^4 (filled diamond) in the $\log U$ version. The solid line is that of the $\hat{\text{MOM}}$ scheme which is singular at $\sim_{\text{MS}} 0.35 \text{ GeV}$.

as $\propto (qa)^{2(1+\gamma_g)}$. Thus,

$$s(q^2) = \frac{g_0^2}{4} Z_A(q^2) G(q^2)^2, \quad (qa)^{2(1+\gamma_d+2\gamma_g)} : \quad (10)$$

The lattice size dependences of the exponents γ_d and γ_g are summarized in Table II. Although the exponent depends on lattice size, the infrared power dependence of the running coupling is stable and the lattice data are qualitatively the same as the results of hypothetical lepton decay [32], but about factor 3 smaller than the Dyson-Schwinger approach [33].

The QCD running coupling in MR truncation scheme of DSE was parametrized as

$$s(q^2) = (t \frac{2}{QCD})^2 = \frac{1}{c_0 + t^2} (c_0 + \frac{4}{\log t} (\frac{1}{t_0} - \frac{1}{t-1})) t^2 \quad (11)$$

where $t = q^2 = \frac{2}{QCD}$ [16].

Phenomenologically fitted QCD from MS_z is about 710 MeV , but the value depends on the number of quarks and in the quenched approximation the choice is not appropriate. We choose as [16], $QCD = 330 \text{ MeV}$. The infrared fixed point t_0 is expressed as an analytic function of $\gamma_d = \gamma_g$, and [17] claims that when two-loop squint diagrams are included, possible solutions exist only for γ_d in the range $[0.17; 0.53]$. Since γ_d depends on lattice size, we treat it as a fitting parameter and take $\gamma_d = 0.2$ and $t_0 = 1.1$ for the sample average, $\gamma_d = 0.24$ and $t_0 = 1.4$ for the exceptional sample. We choose parameter $c_0 = 30$ which is double of the value that is adopted in the DSE calculation [16]. The momentum dependence of Eq.(11) with $\gamma_d = 0.20$ is shown by the short dashed line in Fig.5. The DSE results and lattice data in which the ghost propagator of our average is replaced by that of the I_A copy and the width $\gamma_d = 0.24$ are also shown in the same figure.

In Fig.6, data points of $\ell = 64, 48^4$ lattice [5, 7] as a function of logarithm of momentum $\log_{10} q(\text{GeV})$ are added and compared with this DSE and the contour improved perturbation method [7, 23]. In high momentum region our data is below DSE results, but we can fit the lattice data by the contour improved perturbation method with $\beta = e^{70=6} \sim \frac{1}{M_S}$ (dotted line).

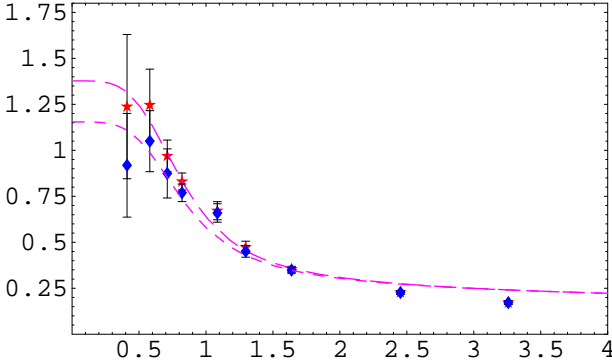


FIG. 5: The running coupling $s(q)$ as a function of momentum $q(\text{GeV})$ of the $\ell = 64, 56^4$ lattice using the ghost propagator of the IA copy (star) and that of the average (diamond). The DSE approach with $\beta = 0.24$ (long dashed line) and that with $\beta = 0.20$ (short dashed line) are also plotted.

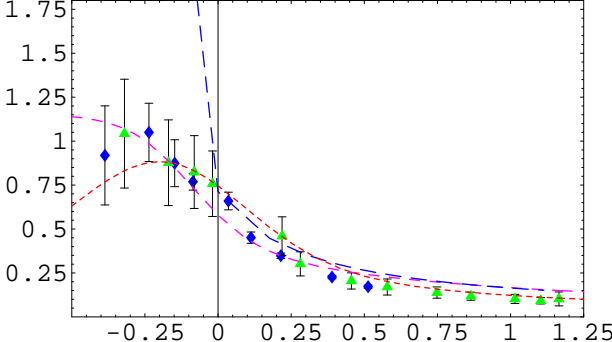


FIG. 6: The running coupling $s(q)$ as a function of logarithm of momentum $\log_{10} q(\text{GeV})$ of the $\ell = 64, 56^4$ (diamond) and 48^4 (triangle) lattice using the ghost propagator of the same average. The DSE approach with $\beta = 0.20$ (dashed line), contour improved perturbation method using $e^{70=6} \sim \frac{1}{M_S}$ (dotted line) are also plotted. The infrared divergent dashed line is the result of MOM scheme.

III. COMPARISON WITH DSE AND ERGE

In the DSE approaches, infrared power behavior and specific relation between the exponent of the ghost propagator and the gluon propagator is assumed. In the

ERGE, flow equation in terms of the effective average action where is the infrared cut-off scale is considered [29, 30, 31]. In a recent work four point vertices in addition to the two point vertices are incorporated and the running coupling was calculated via

$$(q^2) = \frac{g^2(0)}{4 f_Z(q^2; !0) f_G(q^2; !0)} \quad (12)$$

where $f_Z(q^2; !)$ and $f_G(q^2; !)$ are gluon and ghost propagator function, respectively. They are related to the gluon and ghost propagator as

$$D_A(q^2) = (q^2 - q^2) \frac{1}{q^2 f_Z(q^2; !0)} \quad (13)$$

and

$$D_G(q^2) = \frac{1}{q^2 f_G(q^2; !0)} \quad (14)$$

The infrared exponent obtained in this analysis turned out to be $\alpha = 0.146$ in contrast to the DSE approach which suggested $\alpha = 0.5$. The infrared fixed point $q^2 = 4.70$ was predicted which is about factor 3 larger than our lattice simulation.

Bloch [16, 17] included the squint diagram in the DSE and proposed renormalization group invariant truncation scheme. We summarize his approach and compare our lattice results with the theory in this subsection.

The quark propagator in Euclidean momentum state is expressed as [16, 24]

$$\frac{1}{iq - A(q^2) + B(q^2)} = \frac{Z(q^2)}{iq + M(q^2)} \quad (15)$$

and $M(q^2) = B(q^2) = A(q^2)$ is proportional to the quark condensate at large q^2 :

$$M(q^2) \sim \frac{4}{3q^2} \left(\frac{s(q^2)}{s(0)} \right)^{d_m} h(q^2) \quad (16)$$

where $d_m = 12 - (33 - 2N_f)$. Here the number of flavor $N_f = 0$ in the quenched approximation.

The quark field is renormalized as

$$Z(q^2; \beta^2) = Z_2(\beta^2; \beta^2) Z_R(q^2; \beta^2) \quad (17)$$

where Z_R is the renormalized quark dressing function, Z_2 is the quark field renormalization constant and at the renormalization point. We define $Z_R(x) = Z_R(x; \beta^2)$ and $Z_R(\beta^2) = 1$ and $m = M(\beta^2)$. In the DSE [17], m is chosen to be $m_{QCD} = 330 \text{ MeV}$. In the quenched lattice simulation, factorization of the gluon field renormalization is approximately satisfied at $q^2 = 2 \text{ GeV}$.

The renormalized quark dressing function $Z_R(q)$ and the quark mass function $M(q)$ can be calculated by a coupled equation once the running coupling $s(q^2)$ is given [16]. The quark mass function at the origin $M(0)$ is a

function of the parameter c_0 and our fitted value $c_0 = 30$ yields

$$M(0)' 1.27_{\text{QCD}} = 0.419 \text{ GeV} : \quad (18)$$

This value is consistent with the result of quark propagator in quenched lattice Landau gauge simulation [34] extrapolated to 0 momentum. The quark condensate h is estimated as $(0.70_{\text{QCD}})^3$ which is compatible with the recent analysis of quenched lattice QCD [35].

IV. DISCUSSION AND OUTLOOK

We observed that the 1-d FT of gluon propagator of the I_A copy has an axis along which the reaction positivity is manifestly violated. The average of Cartan subalgebra components of K ugo-Ojima parameter along this specific axis becomes consistent to $c = 1$. The 1-d FT of the gluon propagator along the diagonal direction in the lattice is also performed by using the analytical expression of the gluon dressing function in MOM scheme for $q > 1 \text{ GeV}$ and numerical interpolation for $0 < q < 1 \text{ GeV}$. Since reaction positivity violating axis in the average does not coincide with the diagonal axis, violation of reaction positivity is very weak, although the quantitative feature is sensitive to the dressing function near $q = 0$.

When the QCD running coupling in the infrared region is thought to be divergent, the dynamical chiral symmetry breaking which is related to the instanton effect was thought to be irrelevant to confinement [15]. Our lattice data of running coupling is qualitatively similar to that assumed in the dynamical chiral symmetry breaking.

In passing, we compare running coupling measured in other lattice simulations. Our group measured the running coupling with use of U linear gauge-fixing and from triple gluon vertex. The running coupling turned out to behave as $\sim p^4$ in the infrared and above 0.8 GeV the data are consistent with ours. They analyzed the infrared behavior in the instanton liquid model [36]. Running coupling above 0.2 GeV in instanton scheme was measured by the DESY group [37], and the value in infrared is about factor 3 larger than ours but consistent with the results of [38] in $SU(2)$ lattice simulation.

However, we observe inconsistency in the lattice data of Tuebingen group ($16^3 \times 32$) and those of Sao Carlos group (26^4) shown in [38]. The ghost propagator of Sao Carlos group is consistent to ours but that of Tuebingen group is more singular than ours. Our gluon propagator at high momentum region is consistent to Tuebingen, but below 1 GeV our data is more enhanced than that of Tuebingen. The gluon propagator of Sao Carlos group in [38] is similar to their ghost propagator and at $q = 1 \text{ GeV}$ it

is about factor 9 larger than their previous data [39] and factor 2.5 larger than ours. Despite inconsistency in the ghost and the gluon propagator, the running coupling of Sao Carlos and Tuebingen apparently coincide and larger than ours by about factor 3.

We note that the Tuebingen and DESY group choose one axis longer than the others, which could cause the singularity of the ghost propagator stronger than ours. We remark also the ghost propagator in U linear gauge fixing is larger than that of $\log U$ and the running coupling becomes larger by about 20% in $SU(2)$ and in $SU(3)$ [18].

In the study of instantons, Nahm conjectured that Gribov copies cannot tell much about confinement [4]. We showed that the dynamical chiral symmetry breaking and confinement can be explained by using the same running coupling which has the infrared fixed point $\alpha' = 1.5$ and the Gribov copy tells much about chiral symmetry breaking and confinement.

We observed that there are samples whose 1-D FT of the gluon propagator transverse to a lattice axis manifestly violates reaction positivity. The direction of the reaction positivity violating axis appears randomly and so there is no symmetry breaking in sample average. We observed in the 56^4 lattice, an exceptional Gribov copy which has large K ugo-Ojima parameter. It is nothing but a sample in the local minimum and how weight of such samples as I_A changes in the larger lattices and how they should be weighted so that the correct continuum limit is achieved are future problems [3].

In a study of gauge fixing action for lattice gauge theory, Golterman and Shamir [40] proposed a Beken-Rouet-Stora-Tyutin (BRST) invariant gauge fixing by adding irrelevant terms to the ordinary gauge fixing action $S_{\text{gf}} = (\partial A)^2$. Due to this modification, condensation of vector field h_A ($=$ constant for all A) occurs and the phase which is called directional ferromagnetic (FMF) phase was predicted. Our simulation is done by simple Wilson action and there is no direct proof that the I_A copy is a better sample in BRST point of view. Appearance of larger L_2 norm of the I_A copy than the I_B copy and the shift in the coordinate space gluon propagator of I_A from I_B in the 56^4 lattice may suggest complexity of the infrared features of the Landau gauge QCD.

Acknowledgments

S.F. thanks K.-I. Kondo for attracting our attention to the ERGE approach. This work is supported by the KEK supercomputing project No. 03-94.

[1] V.N. Gribov, Nucl. Phys. B 1391 (1978).

[2] D. Zwanziger, Nucl. Phys. B 364, 127 (1991), *ibid.* B

[412, 657 (1994).

[3] D. Zwanziger, Phys. Rev. D 69,016002 (2004) ,hep-ph/0303028.

[4] W .Nahm , in IV Warsaw Symp. on Elem. Part. Phys. ed. Z. A. Jluk, p.275 (Warsaw 1981)

[5] H. Nakajima and S. Furui, Lattice '03 proceedings (2003), hep-lat/0309165.

[6] T. Kugo and I. Ojima, Prog. Theor. Phys. Suppl. 66, 1 (1979).

[7] S. Furui and H. Nakajima, Phys. Rev. D 69,074505 (2004),arX iv:hep-lat/0305010.

[8] C D .Roberts and A .W illiams, Prog. Part. Nucl. Phys. 33,477 (1994), arX iv:hep-ph/9403224.

[9] R A lkofer and L. von Smekal, Phys. Rep. 353,281 (2001), arX iv:hep-ph/0007355.

[10] K -I. Kondo, arX iv:hep-th/0303251.

[11] S. M. andelstam , Phys. Rev. D 20,3223 (1979).

[12] N. Brown and M R. Pennington, Phys. Rev. D 39,2723 (1989)

[13] L. von Smekal, A .Hauck, R .A lkofer, Ann. Phys. (N.Y.) 267,1 (1998), arX iv:hep-ph/9707327;

[14] H .Pagels, Phys. Rev. D 19,3080 (1979).

[15] K .H igashijima, Phys. Rev. D 29, 1228 (1984)

[16] J C R . Bloch, Phys. Rev. D 66,034032 (2002),hep-ph/0202073;

[17] J C R . Bloch, Few Body Syst 33,111 (2003).

[18] H Nakajima and S. Furui, Nucl. Phys. B (Proc Suppl) 63A -C ,635, 865 (1999), Nucl. Phys. B (Proc Suppl) 83-84,521 (2000), 119,730 (2003); Nucl. Phys. A 680,151c(2000), arX iv:hep-lat/0006002, 0007001, 0208074.

[19] S. Furui and H . Nakajima, in Quark Con nement and the Hadron Spectrum IV , Ed. W . Lucha and K M . M aung, W orld Scienti c, Singapore, p.275 (2002), hep-lat/0012017.

[20] H . Nakajima and S. Furui, in Strong Coupling Gauge Theories and Elective Field Theories, Ed. M . Harada, Y . K ikukawa and K . Yamawaki, W orld Scienti c, Singapore, p.67 (2003), arX iv:hep-lat/0303024.

[21] P M Stevenson, Phys. Rev. D 23, 2916 (1981);

[22] G .G runberg, Phys. Rev. D 29, 2315 (1984);

[23] D M .H owe and C J. M axwell, hep-ph/0204036 v2.

[24] C S. Fischer and R . A lkofer, Phys. Rev. D 67,094020 (2003).

[25] M . Stingl, Phys. Rev. D 34,3863 (1986),Z . Phys. A 353,423 (1996).

[26] D B .Leinweber, J.I. Skullenud, A G .W illiams and C . Parrinello, Phys. Rev. D 60,094507 (1999); ibid Phys. Rev. D 61,079901 (2000).

[27] K . Van A coleyen and H . Verschelde, Phys. Rev. D 66,125012 (2002),arX iv:hep-ph/0203211 .

[28] H .Suman and K .Schilling, Phys. Lett.B 373,314 (1996)

[29] C .W etterich, Phys. Lett.B 301,90 (1993).

[30] U .E llwanger, M .H irsch and A .W eber, Eur. Phys. J.C 1, 563 (1998).

[31] J. K ato, arX iv:hep-th/0401068.

[32] S J. B rodsky, S. M enke and C .M erino, Phys. Rev. D 67,055008 (2003), arX iv:hep-ph/0212078 v3.

[33] C S. Fischer, R . A lkofer and H . Reinhardt, hep-ph/0202195.

[34] F D R Bonnet, P O Bowman, D B Leinweber, A G W illiams and J B Zhang, Phys. Rev. D 65,114503 (2002).

[35] D B ecirevic and V .Lubicz, arX iv:hep-ph/0403044

[36] Ph. Boucaud et al, arX iv:hep-ph/0212192.

[37] A .R ingwald and F .Schrempp, arX iv:hep-lat/9903039.

[38] J R C Bloch, A .Cucchieri, K Langfeld and T M endes, Nucl. Phys. B (Proc. Suppl) 119,736 (2003); arX iv:hep-lat/0209040 v2.

[39] A .Cucchieri, T .M endes and D .Zwanziger, Nucl. Phys. B (Proc. Suppl) 106,697 (2002), arX iv:hep-lat/0110188.

[40] M F L .Golterman and Y . Shamir, Phys. Lett. B 399,148 (1997), arX iv:hep-lat/9608116 v2.